Complexes of Rhodium(I) and Iridium(I) with the Chiral Tridentate Phosphane Pigiphos: Structure and Reactivity Studies

Lukas Hintermann,[a] Mauro Perseghini,[a] Pierluigi Barbaro,*[b] and Antonio Togni*[a]

Keywords: Ferrocenyl ligands / Phosphanes / Iridium / Rhodium / Chiral ligands

The chiral ferrocenyltriphosphane Pigiphos [bis{(*S*)-1-[(*R*)-2-(diphenylphosphanyl)ferrocenyl]ethyl}cyclohexylphosphane] forms four-coordinate complexes with Ir^I and Rh^I. The tridentate ligand assumes different conformations in the derivatives [Rh(CO)(Pigiphos)]OTf (**4**) and [IrCl(Pigiphos)] (**1b**), the latter also showing a drastic deviation from the square-planar geometry. Reactivity studies have focussed on the more reactive **1b**. The HCl and O_2 adducts have been characterized in solution.

Introduction

Chiral tridentate phosphanes and their transition metal complexes are rare.[1] We have previously described the chiral tridentate ferrocenylphosphane (*S*,*R*)-Pigiphos = bis{(*S*)-1-[(*R*)-2-(diphenylphosphanyl)ferrocenyl]ethyl}-cyclohexylphosphane (Scheme 1) and its complexes with palladium, nickel and ruthenium.[2] An element of design of Pigiphos is its simple synthetic accessibility (one step from commercially available materials),[2a] thus giving the possibility of varying the steric and electronic properties of the ligand according to a modular approach. Pigiphos forms two six-membered chelate rings when coordinating as a tridentate ligand and is thus best suited for both equatorial and facial arrangements around a transition metal atom, although partial hemilability cannot be excluded.

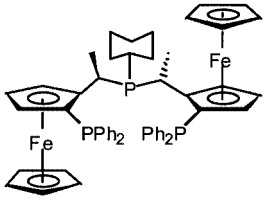

Scheme 1. (*S*,*R*)-Pigiphos

We were able to show that [*fac*-Ru{(*S*,*R*)-Pigiphos}$(CH_3CN)_3$]$(PF_6)_2$ is a catalyst for the enantioselective transfer-hydrogenation of *i*PrOH to acetophenone where *ee* values up to 71.7% could be obtained.[2b] Furthermore, cationic complexes of rhodium(III) and nickel(II) were prepared and their activity as acetalization catalysts was demonstrated.[2c] The synthesis of additional complexes with the unique Pigiphos ligand thus seemed worthwhile in order to explore its coordination chemistry and to find reactive complexes with possible application as catalysts.

The recent findings from our laboratory and from Tani's research group that highly reactive dinuclear iridium(I) complexes with chelating diphosphanes $[Ir_2Cl_2(PP)_2]$ (PP = Josiphos, Xyliphos, BINAP, bpbp) oxidatively add water[3,4] and methanol[4] pointed our attention towards low-valent group-9 species. It seemed that Pigiphos as an electron-rich tridentate ligand should give rise to similar reactivity.

In this paper we describe the synthesis of the reactive mononuclear complexes [RhCl{(*S*,*R*)-Pigiphos}] (**1a**) and [IrCl{(*R*,*S*)-Pigiphos}] (**1b**), and we report on several aspects of their coordination chemistry, including cationic solvento complexes, carbonyl complexes, and their reaction with molecular oxygen. The potential for oxidative addition of small molecules to the iridium(I) complex was investigated. X-ray structures have been determined for **1b** and for [Rh(CO){(*S*,*R*)-Pigiphos}]OTf (**4**)

Results and Discussion

Synthesis and Characterization of the Rh^I and Ir^I Complexes 1, 2, 4

Mononuclear, four-coordinate complexes of the general formula [MX(Pigiphos)]Y were prepared in good yields with M as Rh^I or Ir^I (Scheme 2). The neutral chloro complexes **1a** and **1b** were obtained by a ligand-exchange reaction using $[Rh_2Cl_2(COD)_2]$ or $[Rh_2Cl_2(C_2H_4)_4]$ and

[a] Department of Chemistry, Swiss Federal Institute of Technology,
ETH Hönggerberg, 8093 Zürich, Switzerland
Fax: (internat.) + 41-1/632-1310
E-mail: togni@inorg.chem.ethz.ch
[b] ISSECC − CNR,
Via Jacopo Nardi 39, 50132 Firenze, Italy
E-mail: pigi@fi.cnr.it

$[Ir_2Cl_2(COE)_4]$ (COE = cyclooctene) or $[IrCl(C_2H_4)_4]$, respectively. The cationic derivatives **2a**, **2b** and **4** were obtained by halogen abstraction from the corresponding chloro complexes, using a chloride scavenger.

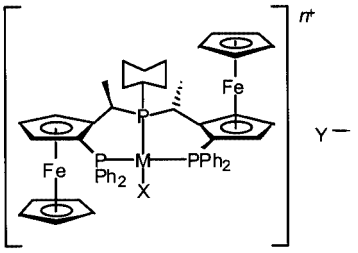

M = Rh, X = Cl, *n* = 0 (**1a**)
M = Ir, X = Cl, *n* = 0 (**1b**)
M = Rh, X = CH_3CN, *n* = 1, Y = PF_6 (**2a**)
M = Ir, X = CH_3CN, *n* = 1, Y = PF_6 (**2b**)
M = Rh, X = CO, *n* = 1, Y = OTf (**4**)

Scheme 2. Sketch of the complexes **1**, **2**, **4**

With the exception of chlorinated solvents, all complexes are fairly stable in solution in deaerated, noncoordinating solvents. The solid-state IR spectra of the acetonitrile and carbonyl adducts [**2a**: ν(C−N) 2317 cm^{-1}; **4**: ν(C−O) 2020 cm^{-1}] show absorptions characteristic of coordinated CH_3CN[5−7] and CO[5,6,8] molecules. The $^{31}P\{^1H\}$ NMR spectroscopic data for the complexes are reported in Table 1, whereas selected ^1H NMR spectroscopic data are reported in the Exp. Sect.

The ^{31}P NMR spectral parameters are consistent with the presence of two diastereotopic ferrocenyl units with $^2J_{P_AP_B}$ coupling constants (from 131.8 to 287.0 Hz) indicative of *trans*-Ph_2P groups in each compound.[9] The complexes are slightly fluxional on the NMR time scale at room temperature, as shown by a moderate broadening of the $^{31}P\{^1H\}$ resonances. However, a slow-motion regime is attained by all compounds to give well-resolved patterns on lowering the temperature to 233−223 K. An analogous ^{31}P NMR behavior has been previously reported for the parent square-planar Pigiphos Pd^{II} and Ni^{II} complexes.[2a] These findings can be attributed to the presence of a conformational equilibrium within the six-membered chelate rings in the complexes. The dynamics of the process have been investigated in detail for complex **1b** (see below). In the rhodium complexes, the trend observed for the $^1J_{RhP}$ coupling constants can be rationalized on the basis of the *trans* influence of the coligands, which decreases in the order CyP ≈ CO > CH_3CN > Cl.[9b,10−12] Indeed, the $^1J_{RhP_A}$ and $^1J_{RhP_B}$ coupling constants of the two *trans*-Ph_2P phosphorus atoms are invariably smaller than the $^1J_{RhP}$ constant for the central CyP phosphorus atom. Consistently, this latter increases in going from **4** (121 Hz) to **2a** (163 Hz), to **1a** (173 Hz) (i.e. from *trans* to CO, CH_3CN, Cl).

The observed ^1H NMR spectral parameters, although in line with two diastereotopic ferrocenyl units, are rather routine and do not deserve any particular comment.

Solid-State Structure of 4

A single-crystal X-ray diffraction analysis carried out on **4** shows that the molecular structure consists of complex

Table 1. $^{31}P\{^1H\}$ NMR data for the Pigiphos complexes

Complex[a]	Compd.	(Cy)P	(Ph)P_A	(Ph)P_B
[(*S*,*R*-Pigiphos]RhCl	**1a**[b]	79.40 (dt) $^2J_{PP}$ = 41.4, $^1J_{PRh}$ = 172.9	17.04 (br. d)	16.48 (br. d)
	1a[c][d]	79.94 (dt) $^2J_{PP}$ = 42.1, $^1J_{PRh}$ = 173.3	17.90 (ddd) $^2J_{P_AP_B}$ = 131.8, $^1J_{P_A}$ = 81.8	17.90 (ddd) $^1J_{P_B}$ = 81.8
[{(*S*,*R*)-Pigiphos}Rh(CH_3CN)]$^+$	**2a**[c]	84.04 (dt) $^2J_{PP}$ = 44.1, $^1J_{PRh}$ = 162.7	24.14 (ddd) $^2J_{P_AP_B}$ = 280.5, $^1J_{P_A}$ = 135.8	19.21 (ddd) $^1J_{P_B}$ = 128.1
[(*S*,*R*)-Pigiphos]Rh(O_2)Cl	**3a**[b]	66.21 (dt) $^2J_{PP}$ = 22.4, $^1J_{PRh}$ = 122.1	16.14 (dt) $^1J_{P_A}$ = 134.8	1.18 (dt) $^1J_{P_B}$ = 134.8
[{(*S*,*R*)-Pigiphos}Rh(CO)]$^+$	**4**[c]	64.23 (ddd) $^2J_{PP_A}$ = 37.1, $^2J_{PP_B}$ = 47.0, $^1J_{PRh}$ = 121.9	21.98 (ddd) $^2J_{P_AP_B}$ = 238.3, $^1J_{P_A}$ = 119.3	15.4 (br. m)
	4[c][e]	63.64 (ddd) $^2J_{PP_A}$ = 34.4, $^2J_{PP_B}$ = 50.3, $^1J_{PRh}$ = 120.4	22.07 (ddd) $^2J_{P_AP_B}$ = 235.8, $^1J_{P_A}$ = 118.7	13.02 (ddd) $^1J_{P_B}$ = 116.5
[(*R*,*S*)-Pigiphos]IrCl	**1b**[f][g]	44.02 (br. t) $^2J_{PP}$ = 26.0	11.3 (br. s) (2P)	
[{(*R*,*S*)-Pigiphos}Ir(CH_3CN)]$^+$	**2b**[f][h]	46.60 (t) $^2J_{PP}$ = 27.0	15.54 (dd) $^2J_{P_AP_B}$ = 287.0	8.51 (dd)
[(*R*,*S*)-Pigiphos]Ir(O_2)Cl	**3b**[f,g]	19.23 (t) $^2J_{PP}$ = 17.2	−20.7 (dd) $^2J_{P_AP_B}$ = 22.4	−34.3 (dd)
[{(*R*,*S*)-Pigiphos}IrClH]$^+$	**5**[b][m]	41.7 (t) $^2J_{PP}$ = 13.4	14.51 (bd) $^2J_{P_AP_B}$ = 328	9.22 (bd)
[(*R*,*S*)-Pigiphos]IrCl_2H	**6**[b,m]	17.04 (t) $^2J_{PP}$ = 17.7	−2.01 (dd) $^2J_{P_AP_B}$ = 400.1	−30.93 (dd)
[(*R*,*S*)-Pigiphos]IrClH_2	**7**[b,f]	15.0 (br. s)	6.53 (dd) $^2J_{PP_A}$ = 20.3, $^2J_{P_AP_B}$ = 347.0	−9.52 (dd) $^2J_{PP_B}$ = 21.0

[a] Chemical shifts in ppm, coupling constants in Hz. 202.47 MHz, 294 K. Abbreviations: s, singlet; d, doublet; t, triplet; m, multiplet; br., broad. [b] C_6D_6. [c] CD_3COCD_3. [d] 233 K. [e] 223 K. [f] 121.5 MHz. [g] [D_8]Toluene. [h] CD_3CN. [m] 101.3 MHz.

cations $[Rh(CO)\{(S,R)\text{-Pigiphos}\}]^+$ and OTf^- anions. An ORTEP view of the cation is shown in Figure 1 while selected bond lengths and angles are reported in Table 2.

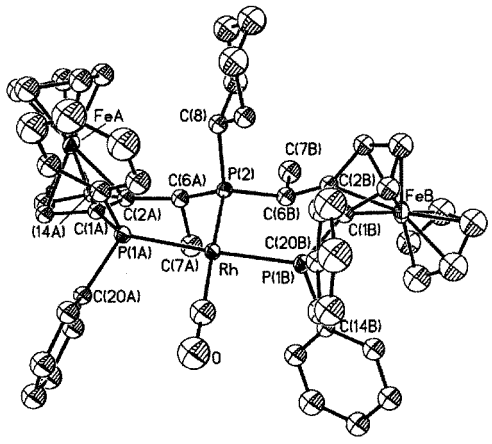

Figure 1. ORTEP drawing of the complex cation $[Rh(CO)\{(S,R)\text{-Pigiphos}\}]^+$ in **4**

The coordination around the metal center is approximately square-planar in which the carbonyl ligand and the CyP P(2) atom are mutually *trans*. The distortions from the idealized geometry are represented by the displacements of the Rh and C(26) atoms from the plane containing the three phosphorus atoms (−0.182 and −0.622 Å, respectively), as well as by the value of the bond angles at the metal (87.4−94.0°). However, considering the best idealized coordination plane of Rh (maximum deviations of the donor atoms 0.152 to −0.179 Å) one can observe that: (i) one of the unsubstituted Cp rings and the two methyl groups lie below this plane, whereas the second Cp ring and the cyclohexyl group are above, (ii) the four phenyl rings are pairwise above and below the plane, thus assuming an overall pseudo-C_2 symmetry, (iii) the couple of "C_2-symmetry-related" phenyl rings, identified by the C(14A) and C(14B) *ipso*-carbon atoms, face an observer lying on the C(26)−P(2) axis. Although both six-membered chelate rings adopt a distorted boat conformation in **4**, their geometry is markedly different. This is shown by the different relative positions of the two methyl groups [cf. the torsion angles C(1B)−C(2B)−C(6B)−C(7B) = −164.8(8)° and C(1A)−C(2A)−C(6A)−C(7A) = 95.7(11)°], as well as by the conformation of the two alkyl side chains [cf. the torsion angles C(1B)−C(2B)−C(6B)−P(2) = 62.7(10)° and C(1A)−C(2A)−C(6A)−P(2) = −26.4(13)°]. Furthermore, the P(1A) phenyl rings are closer to an axial/equatorial arrangement with respect to the coordination plane of Rh than those bonded to P(1B) [cf. the torsion angles C(26)−Rh−P(1A)−C(14A) = 90.3(7)°, C(26)−Rh−P(1A)−C(20A) = −22.3(7)°, C(26)−Rh−P(1B)−C(20B) = −59.1(7)°, C(26)−Rh−P(1B)−C(14B) = 56.7(7)°]. The Rh−C(26)−O angle (178.8°) as well as the C(26)−O (1.134 Å) and Rh−C(1) (1.849 Å) distances are in the range commonly observed for other square-planar (carbonyl)Rh^I complexes.[13,14] The overall conformation of the Pigiphos ligand in **4** closely resembles that already described for the square-planar cation complex $[PdCl\{(S,R)\text{-Pigiphos}\}]^+$.[2a]

Solid-State Structure of 1b·2(C_6H_6)

Compound **1b**·2(C_6H_6) was characterized by X-ray diffraction analysis. Selected bond lengths and angles are reported in Table 3. An ORTEP drawing is depicted in Figure 2.

Table 3. Selected bond lengths [Å] and angles [°] for $[IrCl\{(R,S)\text{-Pigiphos}\}]\cdot 2(C_6H_6)$

Ir−Cl	2.3997(17)	Ir−P(1A)	2.2714(16)
Ir−P(2)	2.2123(17)	Ir−P(1B)	2.2581(18)
Cl−Ir−P(2)	166.79(6)	P(1A)−Ir−P(1B)	154.29(6)
P(1A)−Ir−P(2)	90.73(7)	P(1B)−Ir−P(2)	95.82(7)
Cl−Ir−P(1A)	91.73(7)	Cl−Ir−P(1B)	87.53(7)

The coordination around Ir is approximately square-planar with the chlorine atom and the CyP(2) group *trans* to each other. However, the displacement of the iridium and chlorine atoms above the plane containing the three phosphorus atoms (0.450 and 1.462 Å, respectively) and the bond angles around the metal center (87.50−95.82°) show that the degree of distortion of this complex is larger than for the cation $[Rh(CO)\{(S,R)\text{-Pigiphos}\}]^+$ in **4**. In addition, the overall arrangement of the Pigiphos ligand is markedly different from that observed in **4** and in $[PdCl\{(S,R)\text{-Pigiphos}\}]^+$.[2a] Thus, both methyl groups are below the coordination plane, no pseudo-C_2 symmetry is shown by the phenylphosphanyl groups, and no specific axial/equatorial arrangement is adopted by the phenyl rings [cf. the torsion angles Cl−Ir−P(1B)−C(14B) = 65.7(3)°, Cl−Ir−P(1B)−C(20B) = −53.0(3)°, Cl−Ir−P(1A)−C(14A) = 71.3(3)°, Cl−Ir−P(1A)−C(20A) = −47.1(3)°]. The unusual

Table 2. Selected bond lengths [Å] and angles [°] for the cation $[Rh(CO)\{(S,R)\text{-Pigiphos}\}]^+$ in **4**

Rh-P(1B)	2.302(3)	O−C(26)	1.134(16)
Rh−P(1A)	2.305(3)	Rh−C(26)	1.849(14)
Rh−P(2)	2.318(3)		
C(26)−Rh−P(1B)	86.9(4)	C(26)−Rh−P(2)	170.7(6)
C(26)−Rh−P(1A)	89.9(4)	P(1B)−Rh−P(2)	93.97(11)
P(1B)−Rh−P(1A)	169.45(12)	P(1A)−Rh−P(2)	90.77(11)
Rh−C(26)−O	177.0(6)		
C(1B)−C(2B)−C(6B)−P(2)	62.7(10)	C(1A)−C(2A)−C(6A)−P(2)	−26.4(13)
C(1B)−C(2B)−C(6B)−C(7B)	−164.8(8)	C(1A)−C(2A)−C(6A)−C(7A)	95.7(11)

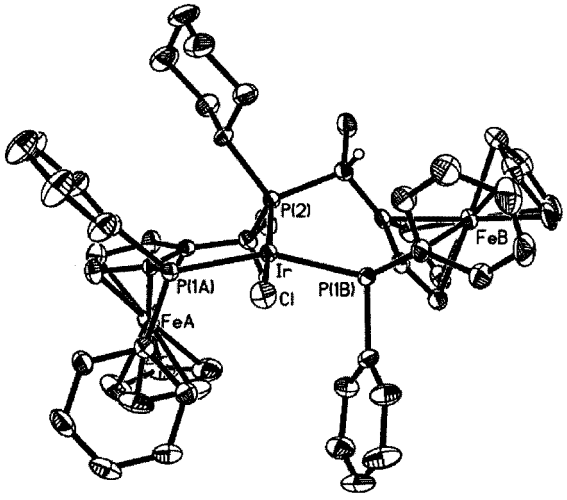

Figure 2. ORTEP view of the complex [IrCl{(*R*,*S*)-Pigiphos}] in **1b**·2(C_6H_6); solvent molecules are omitted for clarity

arrangement of Pigiphos in **1b** is inferred by the different conformation assumed by the two six-membered chelate rings; while the ring incorporating P(1A) can be described as an envelope with five atoms almost lying in a plane [with P(2) out of the plane], the one including P(1B) adopts a distorted boat conformation. It is worth noting that in most of the Josiphos-type ferrocenyldiphosphane complexes the six-membered chelate ring adopts a distorted boat conformation.[3,15,16]

$^{31}P\{^1H\}$ VT NMR Study of Complex 1b

A variable-temperature $^{31}P\{^1H\}$ NMR study was carried out on **1b**. Sections of the $^{31}P\{^1H\}$ NMR spectra of **1b** are shown in Figure 3.

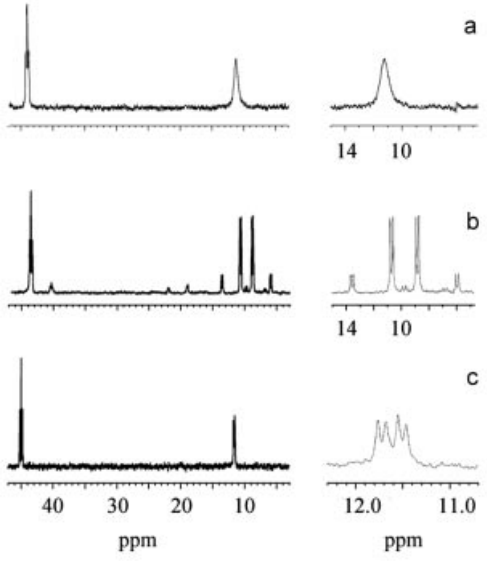

Figure 3. $^{31}P\{^1H\}$ NMR spectra of [IrCl{(*R*,*S*)-Pigiphos}] (**1**) (121.5 MHz, [D_8]toluene): (a) 21 °C, (b) −50 °C and (c) 80 °C

Compared to the parent rhodium complex **1a**, a greater fluxionality is observed for **1b** in room temperature solutions (see Table 1 and Figure 3 a). Indeed, only two resonances are observed at 21 °C, a broad triplet (δ = 44.02 ppm, J = 26 Hz) and a broad singlet (δ = 11.3 ppm), which can be attributed to the central CyP phosphorus atom and to the two terminal Ph_2P atoms, respectively. On lowering the temperature, the latter resonance splits to give a broad ABM spin system, as expected for two diastereotopic diphenylphosphanyl groups. Further cooling causes the signals to sharpen and a second ABM spin system to appear. The spectrum recorded at −50 °C is shown in Figure 3 b. Both sets of resonances (ca. 7:1 ratio, based on ^{31}P NMR integration) show signals characteristic of a central CyP phosphorus atom (major: δ = 43.5 ppm, $^2J_{PP}$ = 25 Hz; minor: δ = 40.3 ppm, $^2J_{PP}$ = 26 Hz) and *trans*-terminal diphenylphosphanyl groups (major: δ = 12.1 and 7.3 ppm, $^2J_{PP}$ = 351 Hz; minor: δ = 8.3 and 20.2 ppm, $^2J_{PP}$ = 358 Hz).[17] According to the solid-state structure, the two spin systems can be attributed to the presence of two isomers of **1b** differing in their conformation − either boat or envelope − of the two six-membered chelate rings. The signals due to the Ph_2P phosphorus atoms are much more differentiated in the minor than in the major isomer (Δδ = 11.9 ppm vs. Δδ = 4.8 ppm). This finding suggests that in the minor isomer the two PPh_2 groups are situated in a quite different chemical environment which results in comparatively unfavorable steric interactions. The observed variable temperature NMR pattern is consistent with an exchange equilibrium between the two isomers, most likely due to a ring-inversion mechanism. Similar ring-inversion processes have been observed previously for six-membered chelate rings in ferrocenyldiphosphane transition metal complexes.[3,15,16] The spectrum recorded at 80 °C is in line with the trend observed at lower temperature. Only one tightly coupled ABM system is found which accounts for the fast interconversion of the two conformers. The spectral parameters (CyP: δ = 44.83 ppm, $^2J_{PP}$ = 8.50 Hz; Ph_2P: δ = 12.02 and 11.19 ppm, $^2J_{PP}$ = 179.9 Hz)[17] indicate that at this temperature the complex attains a time-averaged preferred conformation in which the two terminal phenylphosphanyl groups are located in a similar chemical environment.

Synthesis and Characterization of the (Dioxygen)Rh^{III} and -Ir^{III} Adducts

The (dioxygen)Rh and -Ir adducts **3a** and **3b** were quantitatively obtained by exposure of a C_6H_6 solution of **1a** and **1b** to air, respectively. A color change from orange to yellow (**1a**) or deep red (**1b**) accompanied the O_2 uptake and the solid dioxygen complexes precipitated within a few minutes. The adducts **3** can be treated as formal six-coordinate (peroxo)Rh^{III} and -Ir^{III} complexes obtained by the oxidative addition of O_2 to the Rh^I and Ir^I centers,[18−24] in which an η^2-O_2 ligand is *trans* to the Ph_2P phosphorus atoms. This hypothesis is substantiated by the following experimental observations: (i) the solid-state IR spectra show an absorption characteristic for η^2-O_2 complexes (902 and 829 cm^{-1} ν(O−O) for **3a** and **3b**, respectively);[7,18,19,21−23,25] (ii) no residual paramagnetism is detected by magnetic susceptivity

measurement either in solution or in the solid state; (iii) the MALDI MS analysis carried out under oxygen-free conditions shows peaks consistent with O_2 uptake; (iv) the ^{31}P NMR spectra of **3a** and **3b** show a $^2J_{PP}$ coupling constant (17.2−22.4 Hz, Table 1) indicating a *cis* disposition of the phosphorus atoms and, therefore, a *fac* arrangement of the tridentate ligand; (v) consistent with the increased oxidation state of Rh, the $^1J_{RhP}$ coupling constant of the CyP phosphorus atom (122.1 Hz) in **3a** is smaller than the corresponding constant in the deoxygenated Rh^I complex **1a**;[2c,10,26] (vi) the $^1J_{RhP}$ coupling constant observed for the Ph_2P atoms in **3a** (134.8 Hz) is greater than that observed for the CyP phosphorus atom (122.1 Hz), thus indicating that the two diphenylphosphanyl groups experience a lower *trans* influence, as expected for a *trans*-oxygen donor as compared to a *trans* chloride donor.[12,27,28] The formation of η^2-O_2 complexes by addition of dioxygen to (polydentate phosphane)Rh^I and -Ir^I complexes has a number of precedents in the literature.[7,29−34] It is generally agreed that in the reaction of square-planar d^8 metal complexes with dioxygen to give peroxo adducts, the starting metal complex undergoes a geometrical distortion to allow a better overlap between the metal d orbitals and the π_g* orbital of dioxygen.[20,35,36] The observed *mer*-to-*fac* rearrangement of the Pigiphos ligand accompanying the conversion of **1** to **3** can be explained on this basis.

Oxidative Addition Reactions

The ability of **1b** to react with other small molecules to give the oxidative addition product was examined. In particular, the use of protic reagents with very different acid dissociation constants was investigated.

The reaction with an excess of HBF_4 in benzene solution was monitored by NMR spectroscopy. A quantitative conversion into the complex [IrClH{(*R*,*S*)-Pigiphos}]BF_4 (**5**) was shown and the product was characterized in situ by ^1H and $^{31}P\{^1H\}$ NMR spectroscopy. The value of the $^2J_{PP}$ coupling constant (328 Hz) indicates a *trans* arrangement of the two terminal Ph_2P atoms and, therefore, a *mer* coordination of the tridentate ligand. An apical position can be assigned to the hydride observed in the ^1H NMR spectrum at $\delta = -32.15$ ppm on the basis of the low value of its $^2J_{PH}$ coupling (13.0 Hz).[9]

The reaction of **1b** with HCl gave the complex [$IrCl_2H$\{(*R*,*S*)-Pigiphos\}] (**6**), which was isolated in the solid state and completely characterized in solution by 2D NMR spectroscopy. All resonances were unequivocally attributed by 2D techniques. Once again, the $^{31}P\{^1H\}$ NMR spectroscopic data indicate a *mer* arrangement of the ligand ($^2J_{PP}$ = 440.1 Hz, Table 1). The $^2J_{HP}$ values (16.0 Hz) indicate a *cis* disposition of the hydride ligand [$\delta = -19.48$ (q) ppm] with respect to the phosphorus atoms.[9] An apical position of the hydride ligand can thus be anticipated. It only remained to be seen whether this proton is above or below the coordination plane of the iridium atom. A simple ^1H NOESY measurement addressed this point. The main NOE interactions observed for **6** are represented schematically in Figure 4.

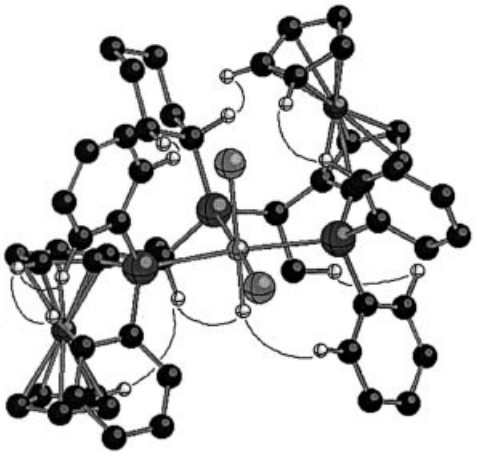

Figure 4. Significant NOEs observed for **6** (C_6D_6, 294 K, 400.13 MHz, drawing generated using the program Ball-and-Stick, see also Figure 5)

The dipolar interaction observed between the hydride atom and one of the α-methyl protons shows the hydride ligand to be located on the side of the plane opposite to that of the cyclohexyl group.

Reaction with methanol did not afford an oxidative addition product. The dihydrido complex [$IrClH_2$\{(*R*,*S*)-Pigiphos\}] (**7**) was obtained and isolated instead. The ^1H NMR spectrum of **7** shows resonances at $\delta = -21.5$ and -7.7 ppm for the two hydride ligands, respectively (see Exp. Sect.). Similar hydride resonances were previously reported for the product from the reaction of [$Ir_2Cl_2(COD)_2$] with tridentate phosphanes in the presence of ethanol/benzene mixtures.[37]

Conclusion

We have shown that Pigiphos behaves as a tridentate ligand with Rh^I and Ir^I forming tetracoordinate complexes. By virtue of a significant distortion of the ideal square-planar geometry, as observed in the solid state and as reflected by the dynamical behavior in solution, the Ir derivative **1b** displays a higher reactivity than **1a** (Rh).

Complex **1b** did not yield OH addition products. This can be explained by the inability of the sterically hindered complex **1b** to generate dinuclear bridged compounds, which seem to stabilize such oxidative addition products. A mononuclear compound would force the lone pairs of the oxygen atom into the electron-rich region of the complex, causing electronic repulsion. The high reactivity of **1b** is now under investigation in order to find possible applications as a catalyst precursor.

Experimental Section

General Remarks: All manipulations were performed under pure nitrogen or argon using standard Schlenk techniques unless other-

wise stated. Freshly distilled solvents were used throughout. Diethyl ether and THF were distilled from Na/benzophenone. Methanol, benzene, toluene, *n*-pentane and *n*-hexane were dried with sodium. CH_3CN was dried with CaH_2. (*S*,*R*)-PPFA and (*R*,*S*)-PPFA,[38] $[RhCl(COD)]_2$,[39] $[RhCl(C_2H_4)_2]_2$,[40] $[RhCl(CO)_2]_2$,[41] and $[IrCl(COE)_2]_2$ [42] were prepared as described previously. The ligands (*S*,*R*)-Pigiphos and (*R*,*S*)-Pigiphos were obtained in better yields (ca. 90%) than previously reported[2a] by using higher concentrations of the starting reagents. All the other chemicals were commercial products of reagent grade and were used as received. All solid compounds were collected on sintered glass frits before being dried in a stream of nitrogen. ^1H, $^{13}C\{^1H\}$ and $^{31}P\{^1H\}$ NMR spectra were recorded with Bruker DPX 250, 300, 400 or Avance DRX-500 spectrometers. ^1H and ^{13}C chemical shifts are relative to tetramethylsilane as external reference or calibrated against solvent resonance. ^{31}P NMR shifts are referenced to external 85% H_3PO_4. The assignments of the signals resulted from ^1H homonuclear decoupling experiments, 2D ^1H COSY and proton-detected ^1H,^{13}C correlations using degassed nonspinning samples. 2D NMR spectra were recorded using pulse sequences suitable for phase-sensitive representations using TPPI. The ^1H,^{13}C correlations[43] were recorded using the standard HMQC sequence with no decoupling during acquisition. Standard pulse sequences were used for ^1H NOESY measurements.[44] Infrared spectra were recorded on Perkin−Elmer Paragon 1000 or 1600 FT-IR spectrometers using samples of KBr or mulled in Nujol between KBr plates. Mass spectrometry was carried out in inert matrices by the Analytical Service of the Organic Chemistry Laboratory, ETH Zürich. Intensities are given as percent relative to the largest peak. Microanalyses were performed by the Microelemental Analysis Service of the Organic Chemistry Laboratory, ETH Zürich. Merck silica gel 60, 230−400 mesh ASTM was used for column chromatography. Thin layer chromatography was performed with Macherey−Nagel Polygram SIL G/UV254 precoated plastic sheets.

[RhCl{(*S*,*R*)-Pigiphos}] (1a). (a): Solid $[Rh_2Cl_2(COD)_2]$ (0.05 g, 0.10 mmol) was added to a solution of (*S*,*R*)-Pigiphos (0.19 g, 0.21 mmol) in absolute ethanol (20 mL). The suspension was refluxed with stirring for 1.5 h causing the precipitation of an orange solid. After cooling the mixture to room temperature, the solid was filtered off and washed with *n*-hexane (20 mL) to give **1a** (0.17 g, 81%) as orange microcrystals. ^1H NMR (C_6D_6, 294 K, 500.13 MHz): δ = 3.69 (quint, $J_{HH} = J_{HP} = 6.9$ Hz, 1 H, C*H*′CH_3), 3.25 (dt, $J_{H,H} = 7.5$, $J_{HP} = 19.4$ Hz, 1 H, C*H*′′CH_3), 1.76 (t, 3 H, CH′C*H*$_3$), 1.80 (dd, $J_{HP} = 4.6$ Hz, 3 H, CH′′C*H*$_3$), 4.60 (s, 1 H, C_5H_3), 4.48 (s, 1 H, C_5H_3), 4.35 (s, 1 H, C_5H_3), 4.30 (s, 1 H, C_5H_3), 4.24 (s, 2 H, C_5H_3), 3.92 (s, 5 H, C_5H_5′), 3.67 (s, 5 H, C_5H_5") ppm. $C_{54}H_{55}ClFe_2P_3Rh$ (1047.01): calcd. C 61.95, H 5.29; found C 61.76, H 5.34. **(b):** Solid $[Rh_2Cl_2(C_2H_4)_4]$ (0.04 g, 0.10 mmol) was added to a solution of (*S*,*R*)-Pigiphos (0.19 g, 0.21 mmol) in benzene (20 mL). After stirring for 2 h at room temperature, the orange solution obtained was concentrated to ca. 10 mL under reduced pressure. Addition of *n*-hexane (10 mL) gave **1a** as an orange solid which was filtered off and washed with *n*-hexane (yield 0.10 g, 48%).

[IrCl{(*R*,*S*)-Pigiphos}] (1b): Solid $[Ir_2Cl_2(COE)_4]$ (COE = cyclooctene) (1.920 g, 2.143 mmol) was added to a solution of (*R*,*S*)-Pigiphos (3.897 g, 4.289 mmol) in THF (15 mL). After stirring for 2 h, the resulting dark brown solution was freed from undissolved material by decantation. Evaporation of the solvent under high vacuum for 3 h at 70 °C gave an orange crystalline mass. This material was triturated with *n*-hexane (30 mL), filtered, washed with *n*-pentane (50 mL) and dried under high vacuum to give 4.584 g of **1b** (94% yield) as a dark yellow powder. ^1H NMR ([D$_8$]toluene, 294 K, 400.13 MHz): δ = 8.15 (br. s, 2 H, *ortho*-Ph), 8.10−8.03 (m, 2 H, *ortho*-Ph), 8.03−7.96 (m, 2 H, *ortho*-Ph), 7.86−7.79 (m, 2 H, *ortho*-Ph), 7.18−6.98 (m, 12 H, Ph), 4.34−4.32 (m, 1 H, C_5H_3), 4.23 (br. s, 1 H, C_5H_3), 4.07−4.05 (m, 1 H, C_5H_3), 4.04−4.02 (m, 1 H, C_5H_3), 4.02−3.99 (m, 2 H, C_5H_3), 3.66 (s, 5 H, C_5H_5′), 3.64−3.59 (m, 1 H, C*H*′CH_3), 3.38 (s, 5 H, C_5H_5"), 3.14 (br. s, 1 H, C*H*"CH_3), 2.75 (br. q, $J = 11.0$ Hz, 1 H, CyH), 2.31−2.21 (m, 1 H, CyH), 1.84−1.75 (m, 1 H, CyH), 1.71−1.63 (m, 1 H, CyH), 1.58 (dd, $J = 7.0$, $J = 5.8$ Hz, 3 H, CH_3′), 1.54 (dd, $J = 4.0$, $J = 3.4$ Hz, 3 H, CH_3′′), 1.45−1.26 (m, 2 H, CyH), 1.23−1.16 (m, 3 H, CyH), 1.10−0.86 (m, 2 H, CyH) ppm. $^{13}C\{^1H\}$ NMR ([D$_8$]toluene, 294 K, 62.9 MHz): δ = 137.4, 137.1, 134.9, 134.4, 129.3, 129.2, 128.2, 126.9, 125.4, 99.8 (1 C, C_5H_3), 93.5 (1 C, C_5H_3), 75.3 (1 C, C_5H_3), 73.3 (1 C, C_5H_3), 70.7 (5C, C_5H_5′), 70.6 (5C, C_5H_5"), 69.2 (1 C, C_5H_3), 68.8 (1 C, C_5H_3), 68.1 (1 C, C_5H_3), 67.3 (1 C, C_5H_3), 38.9, (1 C, *C*HCH_3), 35.3 (1 C, α-CH-Cy), 30.3 (1 C, CH_2), 29.8 (1 C, CH_2), 28.0 (1 C, CH_2), 27.5 (1 C, CH_2), 27.2 (1 C, CH_2), 26.3 (1 C, *C*HCH_3), 23.0 (1 C, CH_3), 15.4 (1 C, CH_3) ppm. MS (MALDI): *m*/*z* (%) = 1101 (100) $[M - Cl]^+$, 1018 (22) $[M - Cl - Cy]^+$, 984 (14) $[M - Cl - FeCp]^+$, 919 (15), 902 (16), 838 (14), 804 (16), 725 (16), 711 (17), 634 (28). $C_{54}H_{55}ClFe_2IrP_3$ (1136.32): calcd. C 57.08, H 4.88, P 8.18; found C 57.34, H 5.02, P 8.44.

[Rh{(*S*,*R*)-Pigiphos}(CH$_3$CN)]PF$_6$ (2a): Solid $TlPF_6$ (0.03 g, 0.08 mmol) was added to a solution of **1a** (0.08 g, 0.08 mmol) in acetonitrile (7 mL) and the mixture was stirred for 10 min. After removal of TlCl by filtration, the orange solution obtained was concentrated to ca. half the volume under reduced pressure. Addition of diethyl ether (10 mL) caused the precipitation of an orange solid, which was separated, washed with diethyl ether (40 mL) and dried in vacuo to give 52 mg of **2a** (55% yield). ^1H NMR (CD_3COCD_3, 294 K, 500.13 MHz): δ = 3.68 (dt, $J_{H,H} = 6.8$, $J_{HP} = 19.3$ Hz, 1 H, C*H*′CH_3), 3.42 (quint, $J_{H,H} = J_{HP} = 7.3$ Hz, 1 H, C*H*"CH_3), 1.88 (dd, $J_{HP} = 13.8$ Hz, 3 H, CH′C*H*$_3$), 2.10 (dd, $J_{HP} = 10.4$ Hz, 3 H, CH"C*H*$_3$), 5.09 (s, 1 H, C_5H_3), 4.82 (s, 1 H, C_5H_3), 4.78 (q, 1 H, C_5H_3), 4.76 (s, 1 H, C_5H_3), 4.73 (t, 1 H, C_5H_3) 4.49 (s, 1 H, C_5H_3), 4.09 (s, 5 H, C_5H_5′), 3.87 (s, 5 H, C_5H_5"), 1.68 (s, 3 H, C*H*$_3$CN) ppm. ^{13}C NMR (CD_3COCD_3, 294 K, 125.76 MHz): δ = 1.82 (s, *C*H$_3$CN, $J_{C,H} = 134.4$ Hz) ppm. IR: $\tilde{\nu}$ = 2317 ν(C−N) cm^{-1}. $C_{56}H_{58}F_6Fe_2NP_4Rh$ (1197.57): calcd. C 56.17, H 4.88; found C 56.24, H 4.87.

[Ir{(*R*,*S*)-Pigiphos}(CH$_3$CN)]PF$_6$ (2b): $TlPF_6$ (0.36 g, 1.02 mmol) was added to a solution of **1b** (1.15 g, 1.01 mmol) in CH_3CN (10 mL). After stirring at room temperature for 4 d, the mixture obtained was filtered. Concentration to dryness yielded an orange resin which crystallized on standing. The solid material was powdered and dried under high vacuum (3 d at 50 °C) affording 1.3 g of **2b** (quantitative yield). ^1H NMR (CD_3CN, 294 K, 300.13 MHz): δ = 8.18−8.04 (m, 4 H, Ph), 7.56−7.37 (m, 11 H, Ph), 7.30−7.23 (m, 3 H, Ph), 6.99−6.90 (m, 2 H, Ph), 4.81 (br. s, 1 H, C_5H_3), 4.56−4.51 (m, 2 H, C_5H_3), 4.51−4.49 (m, 1 H, C_5H_3), 4.47 (br. t, 1 H, C_5H_3), 4.26 (br. s, 1 H, C_5H_3), 3.86 (s, 5 H, C_5H_5′), 3.67 (s, 5 H, C_5H_5"), 3.41 (dd, $J = 11.5$, $J = 6.8$ Hz, 1 H, C*H*′CH_3), 3.33 (dd, $J = 11.5$, $J = 7.7$ Hz, 1 H, C*H*"CH_3), 2.36 (br. q, $J = 11.0$ Hz, 1 H, CyH), 2.28 (br. d, $J = 14.0$ Hz, 1 H, CyH), 1.96 (s, 3 H, C*H*$_3$CN), 1.82 (dd, $J = 11.1$, $J = 7.3$ Hz, 3 H, C*H*$_3$′), 1.65 (dd, $J = 13.5$, $J = 6.9$ Hz, 3 H, C*H*$_3$′′), 1.78−1.56 (m, 3 H, CyH), 1.50 (br. d, $J = 11.0$ Hz, 1 H, CyH), 0.16−1.90 (m, 2 H, CyH), 0.68 (br. q, $J = 13.0$ Hz, 1 H, CyH), 0.50 (br. q, $J = 13.0$ Hz, 1 H, CyH), 0.31 (m, 1 H, CyH) ppm. $^{13}C\{^1H\}$ NMR (CD_3CN, 294 K, 62.9 MHz): δ = 121.3 (br. d, $J_{P,C} = 16.0$ Hz, 1 C, CD_3CN), 100.9 (br. d, $J_{P,C} = 21.0$ Hz 1 C, C_5H_3), 93.4 (dd, $J_{P,C} = 20.0$, $J_{P,C}$ =

5.0 Hz, 1 C, C_5H_3), 75.3 (t, $J_{P,C}$ = 3.0 Hz, 1 C, C_5H_3), 74.1 (t, $J_{P,C}$ = 3.0 Hz, 1 C, C_5H_3), 71.6 (s, 5 H, C_5H_5'), 71.3 (s, 5 H, C_5H_5"), 1.8 (s, 1 C, CH_3CN) ppm. $C_{56}H_{58}F_6Fe_2IrNP_4$ (1286.88): calcd. C 52.27, H 4.54, N 1.09; found C 51.78, H 5.00, N 1.04.

[RhCl(O$_2$){(*S*,*R*)-Pigiphos}] (3a): A solution of **1a** (0.05 g, 0.05 mmol) in benzene (5 mL) was stirred in air for 30 min. During this time, yellow microcrystals of **3a** precipitated. Subsequently, they were filtered off and washed with *n*-hexane. Yield: 47 mg (87%). ^{1}H NMR (C_6D_6, 294 K, 500.13 MHz): δ = 4.72 (dt, $J_{H,H}$ = 6.2, J_{HP} = 12.0 Hz 1 H, C*H*′CH$_3$), 3.61 (quint, 1 H, C*H*"CH$_3$, $J_{H,H}$ = J_{HP} = 5.2 Hz), 1.72 (dd, J_{HP} = 10.5 Hz, 3 H, CH′C*H*$_3$), 1.94 (dd, J_{HP} = 9.2 Hz, 3 H, CH"C*H*$_3$), 4.50 (s, 1 H, C_5H_3), 4.48 (s, 1 H, C_5H_3), 4.35 (s, 1 H, C_5H_3), 4.22 (s, 1 H, C_5H_3), 4.18 (s, 1 H, C_5H_3) 3.74 (s, 1 H, C_5H_3), 3.68 (s, 5 H, C_5H_5'), 3.47 (s, 5 H, C_5H_5") ppm. IR: $\tilde{\nu}$ = 902 ν(O−O) cm^{-1}. $C_{54}H_{55}ClFe_2O_2P_3Rh$ (1079.01): calcd. C 60.11, H 5.14; found C 60.33, H 5.01.

[IrCl(O$_2$){(*R*,*S*)-Pigiphos}] (3b): A solution of **1b** (15 mg, 13.2 μmol) in benzene (3 mL) was stirred in air for 5 min yielding **3** as a red precipitate. ^{1}H NMR ([D$_8$]toluene, 294 K, 300.13 MHz): δ = 8.87−8.73 (br. s, 2 H, *ortho*-Ph), 7.84−7.75 (m, 2 H, *ortho*-Ph), 7.69−7.61 (m, 2 H, *ortho*-Ph), 7.59−7.51 (m, 2 H, *ortho*-Ph), 4.26−4.23 (m, 1 H, C_5H_3), 4.22−4.20 (m, 1 H, C_5H_3), 4.13−4.10 (m, 2 H, C_5H_3), 3.95 (t, *J* = 2.4 Hz, 1 H, C_5H_3), 3.87 (t, *J* = 2.7 Hz, 1 H, C_5H_3), 3.41 (s, 5 H, C_5H_5'), 3.37 (s, 5 H, C_5H_5"), 1.67 (dd, *J* = 11.4, *J* = 7.2 Hz, 3 H, CH$_3$′), 1.45 (dd, *J* = 11.4, *J* = 7.2 Hz, 3 H, CH$_3$′′) ppm. MS (MALDI): *m*/*z* (%) = 1168 (20) [M]$^+$, 1152 (20) [M − O]$^+$, 1136.3 (100) [M − O$_2$]$^+$. IR (KBr): $\tilde{\nu}$ = 829 ν(O−O) cm^{-1}.$C_{54}H_{55}ClFe_2IrO_2P_3$ (1168.32): calcd. C 55.52, H 4.74; found C 55.71, H 4.91.

[Rh(CO){(*S*,*R*)-Pigiphos}]OTf (4): Solid [Rh$_2$Cl$_2$(CO)$_4$] (0.06 g, 0.15 mmol) was added to a solution of (*S*,*R*)-Pigiphos (0.30 g, 0.33 mmol) in acetone (10 mL). Solid AgOTf (0.08 g, 0.33 mmol) was added to the resulting solution and CO was bubbled through it for 10 min. The red solution obtained after filtration was concentrated to ca. half the volume under reduced pressure. Addition of *n*-pentane (15 mL) caused the formation of a red oil which crystallized on standing. The solid was washed with *n*-pentane and dried in vacuo to give 114 mg of **4** (64%). ^{1}H NMR (CD_3COCD_3, 294 K, 500.13 MHz): δ = 3.88 (dt, $J_{H,H}$ = 6.4, J_{HP} = 12.4 Hz, 1 H, C*H*′CH$_3$), 3.59 (quint, $J_{H,H}$ = J_{HP} = 7.4 Hz, 1 H, C*H*"CH$_3$), 1.84 (dd, J_{HP} = 14.1 Hz, 3 H, CH′C*H*$_3$), 2.14 (dd, J_{HP} = 11.0 Hz, 3 H, CH"C*H*$_3$), 5.23 (s, 1 H, C_5H_3), 4.96 (s, 1 H, C_5H_3), 4.90 (q, 1 H, C_5H_3), 4.86 (t, 1 H, C_5H_3), 4.81 (s, 1 H, C_5H_3) 4.56 (s, 1 H, C_5H_3), 4.16 (s, 5 H, C_5H_5'), 3.96 (s, 5 H, C_5H_5") ppm. IR: $\tilde{\nu}$ = 2020 ν(C−O) cm^{-1}. $C_{56}H_{55}F_3Fe_2O_4P_3RhS$ (1188.63): calcd. C 56.59, H 4.66; found C 56.63, H 4.64.

[IrClH{(*R*,*S*)-Pigiphos}]BF$_4$ (5): A solution of HBF_4 in diethyl ether (54%, 2 μL, 14.6 μmol) was added to a solution of **1b** (10 mg, 8.8 μmol) in C_6D_6 (1 mL). An NMR analysis showed a quantitative conversion into **5**. ^{1}H NMR (C_6D_6, 294 K, 250.1 MHz): δ = 5.63 (m, 1 H, C_5H_3), 5.50 (m, 1 H, C_5H_3), 4.38 (m, 1 H, C_5H_3), 4.25 (m, 2 H, C_5H_3), 4.21 (s, 6 H, C_5H_5' + C_5H_3), 3.99 (s, 5 H, C_5H_5"), 2.26 (dd, *J* = 13.5, *J* = 7.5 Hz, 3 H, CH$_3$′), 2.05 (dd, *J* = 13.5, *J* = 7.5 Hz, 3 H, CH$_3$′′), −32.15 (br. q, J_{HP} = 13.0 Hz, 1 H, hydride).

[IrCl$_2$H{(*R*,*S*)-Pigiphos}] (6): A solution of HCl in diethyl ether (1 M, 0.1 mL, 100 μmol) was added to **1b** (46 mg, 40.5 μmol), dissolved in benzene (1 mL). After stirring for 3 h, the solution was concentrated to dryness under high vacuum to yield **6** as a yellow solid. ^{1}H NMR (C_6D_6, 294 K, 400.13 MHz, see Figure 5 for the labeling scheme): δ = 8.77 [m, 2 H, H−C(21B), H−C(25B)], 8.66 [m, 2 H, H−C(15B), H−C(19B)], 8.37 [m, 2 H, H−C(21A), H−C(25A)], 8.20 [m, 2 H, H−C(15A), H−C(19A)], 7.39 [m, 2 H, H−C(22A), H−C(24A)], 7.36 [m, 2 H, H−C(16B), H−C(18B)], 7.31 [m, 2 H, H−C(16A), H−C(18A)], 7.26 [m, 1 H, H−C(23A)], 7.24 [m, 1 H, H−C(17A)], 7.20 [m, 1 H, H−C(17B)], 7.11 [m, 2 H, H−C(22B), H−C(24B)], 7.05 [m, 1 H, H−C(23B)], 4.49 [m, 1 H, H−C(5A)], 4.45 [s, 5 H, H−C(1B′) to C(5B′)], 4.36 [m, 1 H, H−C(3A)], 4.26 [m, 1 H, H−C(5B)], 4.22 [m, 1 H, H−C(4B)], 4.07 [m, 1 H, H−C(4A)], 4.03 [m, 1 H, H−C(8)], 4.02 [m, 1 H, H−C(3B)], 3.41 [m, 1 H, H−C(6A)], 3.36 [s, 5 H, H−C(1A′) to H−C(5A′)], 3.23 [m, 1 H, H−C(6B)], 2.67 (m, 1 H, H$_{eq}$−C(9)], 2.49 (m, 1 H, H$_{eq}$−C(13)], 1.86 [m, 1 H, H−C(12)], 1.74 (m, 1 H, H$_{eq}$−C(10)], 1.73 (m, 1 H, H$_{ax}$−C(13)], 1.71 (m, 1 H, H$_{eq}$−C(11)], 1.59 [m, 1 H, H−C(12)], 1.49 (m, 3 H, Me−C(7A)], 1.44 (m, 1 H, H$_{ax}$−C(10)], 1.22 (m, 1 H, H$_{ax}$−C(11)], 1.08 (m, 3 H, Me−C(7B)], 0.93 (m, 1 H, H$_{ax}$−C(9)], −19.48 (q, J_{PH} = 16.0 Hz, 1 H, hydride) ppm. ^{13}C{^{1}H} NMR (C_6D_6, 294 K, 75.5 MHz, see Figure 5 for the labeling scheme): δ = 137.3 [C(21B), C(25B)], 136.9 [C(21A), C(25A)]; 136.3 [C(15A), C(19A)], 134.4 [C(15B), C(19B)], 129.9 [C(17B)], 129.9 [C(23B)], 129.8 [C(23A)], 129.7 [C(17A)], 127.6 [C(16B), C(18B)], 127.4 [C(22A), C(24A)], 127.3 [C(22B), C(24B)], 126.6 [C(16A), C(18A)], 98.8 [d, $J_{P,C}$ = 19.9 Hz, C(2B)], 94.6 [d, $J_{P,C}$ = 15.4 Hz, C(2A)], 75.9 [C(5A)], 72.4 [C(5B)], 71.6 [5C, C(1B′) to C(5B′)], 71.3 [d, $J_{P,C}$ = 7.6 Hz, C(3B)], 71.0 [5C, C(1A′) to C(5A′)], 69.3 [C(3A)], 68.3 [C(4A)], 68.1 [C(4B)], 67.5 [C(1B)], 35.9 [d, $J_{P,C}$ = 25.3 Hz, C(6A)], 34.6 [d, $J_{P,C}$ = 26.0 Hz, C(8)], 30.5 [d, $J_{P,C}$ = 14.0 Hz, C(9)], 29.7 [C(13)], 27.9 [C(12)], 27.1 [C(10)], 27.1 [C(11)], 24.4 [d, $J_{P,C}$ = 32.6 Hz, C(6B)], 23.3 [C(7B)], 16.6 [C(7A)] ppm. IR (KBr): $\tilde{\nu}$ = 2185 ν(Ir−H) cm^{-1}. MS (FAB): *m*/*z* (%) = 1137.5 (100) [M − Cl]$^+$, 1097.4 (20), 1016.4 (53) [M − Cl − CpFe,]$^+$, 981.5. $C_{54}H_{56}Cl_2Fe_2IrP_3$ (1172.78): calcd. C 55.30, H 4.81; found C 57.63, H 5.61.

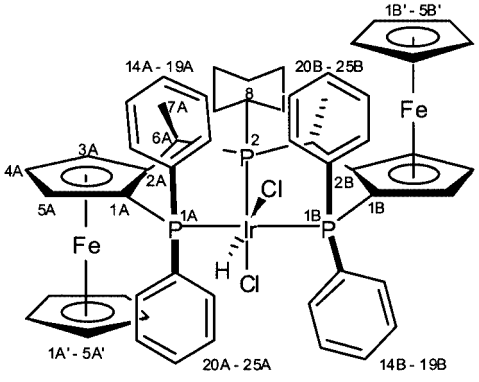

Figure 5. Labeling scheme adopted for the NMR assignment of **6**

[IrClH$_2${(*R*,*S*)-Pigiphos}] (7): A solution of **1b** (34 mg, 29.9 μmol) in benzene/methanol (1:1, v/v; 6 mL) was stirred at room temperature for 11 h. The solvent was evaporated in vacuo and the yellow residue obtained was dissolved in benzene. On addition of *n*-pentane a yellow solid precipitated which was filtered and washed three times with *n*-pentane. Yield: 10 mg (29%). ^{1}H NMR (C_6D_6, 294 K, 300.13 MHz): δ = 4.65 (m, 1 H), 4.58 (m, 1 H), 4.32 (m, 1 H), 4.18 (m, 2 H), 4.10 (m, 1 H), 3.96 (s, 5 H, C_5H_5'), 3.80 (br. *m*, 5 H, C_5H_5"), 3.22 (m, 1 H, C*H*′CH$_3$), 2.56 (br. *m*, 1 H, C*H*"CH$_3$), 1.81 (m, 3 H, CHC*H*$_3$′), 1.78 (m, 3 H, CHC*H*$_3$"), −7.7 (dt, *J* = 123.5, *J* = 16.4, 1 H, hydride), −21.5 (br. m, 1 H, hydride) ppm. MS (FAB): *m*/*z* (%) = 1137.2 (100) [M − Cl]$^+$, 1099.3 (66), 1016.3 (28), 694.7 (13). $C_{54}H_{57}ClFe_2IrP_3$ (1138.33): calcd. C 56.98, H 5.05; found C 56.95, H 5.01.

Table 4. X-ray crystallographic data for compounds **1b** and **4**

	1b	**4**
Empirical formula	C66H55ClFe2IrP3	C56H55F3Fe2O4P3RhS
Formula mass	1280.36	1188.58
Crystal system	orthorhombic	orthorhombic
Space group	*P*212121	*P*212121
a [Å]	9.9347(15)	19.629(6)
b [Å]	21.090(3)	19.713(8)
c [Å]	27.474(4)	13.727(2)
Volume [Å^3]	5756.4(15)	5312(3)
Z	4	4
Density (calculated) [g/cm^3]	1.477	1.486
Absorption coefficient [mm^{-1}]	2.973	1.031
F(000)	2568	2432
Crystal size [mm]	0.82 × 0.26 × 0.12	0.500 × 0.275 × 0.225
θ range [°]	1.22−26.40	2.54−22.47
Index ranges	−12/+12, −26/+26, −25/+34	0/+21, 0/+21, 0/+14
Reflections collected	36365	3844
Independent reflections	11815 [*R*(int) = 0.0486]	3844 [*R*(int) = 0.0000]
Parameters	600	277
Final *R* indices [$I > 2\sigma(I)$]	0.034	0.0515
R indices (all data)	0.074	0.1477
Largest diff. peak and hole [e/Å^3]	1.234 and −1.421	0.716 and −0.557

X-ray Crystallographic Study: Crystals of **1b**·2(C_6H_6) were obtained by slow evaporation of the solvent from concentrated benzene/pentane solutions of **1b** under nitrogen. The X-ray diffraction analysis was performed with exclusion of air with a Siemens CCD SMART area detector system. Selected bond lengths and angles of **1b**·2(C_6H_6) are reported in Table 3. Crystals of **4** suitable for an X-ray diffraction analysis were obtained by recrystallization from acetone/*n*-pentane under a stream of nitrogen. X-ray data were collected at room temperature with an Enraf−Nonius CAD4 diffractometer. Selected bond lengths and angles for **4** are reported in Table 2. A summary of the most important crystal and data collection parameters is given in Table 4 for both compounds. CCDC-186457 (**1b**) and -186458 (**4**) contain the supplementary crystallographic data for this paper. These data can be obtained free of charge at www.ccdc.cam.ac.uk/conts/retrieving.html [or from the Cambridge Crystallographic Data Centre, 12 Union Road, Cambridge CB2 1EZ, UK; Fax: (internat.) + 44-1223/336-033; E-mail: deposit@ccdc.cam.ac.uk].

Acknowledgments

We are grateful to D. Broggini, H. Rüegger and D. Masi for technical assistance. We thank Patrick Dietemann, Laboratorium für Organische Chemie, ETH, for the graphite-assisted laser desorption/ionisation experiments which were performed with a home-built 2-m linear time-of-flight mass spectrometer. Thanks are also due to COST D24 Chemistry Action for financial support.

[1] [1a] F. A. Cotton, B. Hong, *Prog. Inorg. Chem.* **1992**, *40*, 179. [1b] C. R. Johnson, T. Imamoto, *J. Org. Chem.* **1987**, *52*, 2170. [1c] M. J. Burk, R. L. Harlow, *Angew. Chem.* **1990**, *102*, 1511. [1d] M. J. Burk, J. E. Feaster, R. L. Harlow, *Tetrahedron: Asymmetry* **1991**, *2*, 569. [1e] T. R. Ward, L. M. Venanzi, A. Albinati, F. Lianza, T. Gerfin, V. Gramlich, G. M. Ramos Tombo, *Helv. Chim. Acta* **1991**, *74*, 983. [1f] H. Heidel, G. Huttner, L. Zsolnai, *Z. Naturforsch., Teil B* **1995**, *50*, 729. [1g] G. Jia, H. M. Lee, I. D. Williams, *Organometallics* **1996**, *15*, 4235. [1h] Y. Yao, C. J. A. Daley, R. McDonald, S. H. Bergens, *Organometallics* **1997**, *16*, 1890. [1i] H. M. Lee, C. Yang, G. Jia, *J. Organomet. Chem.* **2000**, *601*, 330. [1j] R. B. King, J. Bakos, C. D. Hoff, L. Markó, *J. Org. Chem.* **1979**, *44*, 3095. [1k] H. Heidel, J. Scherer, A. Asam, G. Huttner, O. Walter, L. Zsolnai, *Chem. Ber.* **1995**, *128*, 293.

[2] [2a] P. Barbaro, A. Togni, *Organometallics* **1995**, *14*, 3570. [2b] P. Barbaro, C. Bianchini, A. Togni, *Organometallics* **1997**, *16*, 3004. [2c] P. Barbaro, C. Bianchini, W. Oberhauser, A. Togni, *J. Mol. Cat. A* **1999**, *145*, 139.

[3] R. Dorta, A. Togni, *Organometallics* **1998**, *17*, 3423.

[4] K. Tani, A. Iseki, T. Yamagata, *Angew. Chem. Int. Ed.* **1998**, *37*, 3381.

[5] K. Nakamoto, *Infrared and Raman Spectra of Inorganic and Coordination Compounds*, Wiley, New York, **1986**.

[6] M. Sekine, W. D. Harman, H. Taube, *Inorg. Chem.* **1988**, *27*, 3604.

[7] T. E. Nappier, Jr, D. W. Meek, R. M. Kirchner, J. A. Ibers, *J. Am. Chem. Soc.* **1973**, *95*, 4194.

[8] G. G. Johnston, M. C. Baird, *Organometallics* **1989**, *8*, 1894.

[9] [9a] A. L. Crumbliss, R. J. Topping, "Phosphorus-31 NMR Spectroscopy in Stereochemical Analysis" (Eds.: J. G. Verkade, L. D. Quin), in: *Methods in Stereochemical Analysis 8*, VCH, Weinheim, Germany, **1987**, chapter 15, p. 531. [9b] P. S. Pregosin, R. W. Kunz, in: *^{31}P and ^{13}C NMR of Transition Metal Phosphane Complexes* (Eds.: P. Diehl, E. Fluck, R. Kosfeld), Springer-Verlag, Berlin, **1979**.

[10] D. W. Meek, T. J. Mazanec, *Acc. Chem. Res.* **1981**, *14*, 266.

[11] T. G. Appleton, H. C. Clark, L. E. Manzer, *Coord. Chem. Rev.* **1973**, *10*, 335.

[12] J. G. Verkade, J. A. Mosbo, "Phosphorus-31 NMR Spectroscopy in Stereochemical Analysis" (Eds.: J. G. Verkade, L. D. Quin), in: *Methods in Stereochemical Analysis 8*, VCH, Weinheim, Germany, **1987**, chapter 13, p. 432.

[13] P. R. Sharp, in: *Comprehensive Organometallic Chemistry II* (Eds.: E. W. Abel, F. G. A. Stone, G. Wilkinson), Pergamon, Oxford, U. K., **1995**, vol. 8, chapter 2, p. 138−158.

[14] A. G. Orpen, L. Brammer, F. H. Allen, O. Kennard, D. G. Watson, R. Taylor in *Structure Correlation* (Eds.: H.-B. Bürgi, J. D. Dunitz), VCH, Weinheim, Germany, **1994**, vol. 2, p. 751−857.

[15] A. Togni in: *Organic Synthesis via Organometallics* [OSM5] (Eds.: G. Helmchen, J. Dibo, D. Flubacher, B. Wiese), Vieweg, Braunschweig, **1997**, p. 185−208.

[16] A. Togni, F. Spindler, G. Rihs, N. Zanetti, M. C. Soares, T. Gerfin, V. Gramlich, *Inorg. Chim. Acta* **1984**, *222*, 213.
[17] ABM spin system. Data obtained from computer simulation using the program g NMR ver. 4.1.0, IvorySoft, Cherwell Scientific Publishing, **1995−1999**.
[18] H. Allen, O. Hill, D. G. Tew, "Dioxygen, Superoxide and Peroxide", in: *Comprehensive Coordination Chemistry* (Eds.: G. Wilkinson, R. D. Gillard, J. A. McCleverty), Pergamon Press, Oxford, England, **1987**, vol. 2, p. 315.
[19] L. Vaska, *Acc. Chem. Res.* **1976**, *9*, 175.
[20] M. H. Gubelmann, A. F. Williams, *Struct. Bonding [Berlin]* **1983**, *55*, 1.
[21] *Oxygen Complexes and Oxygen Activation by Transition Metal* (Eds.: A. E. Martell, D. T. Sawyer), Plenum Press, New York, **1988**.
[22] H. Mimoun, "Metal Complexes in Oxidation" in: *Comprehensive Organometallic Chemistry* (Eds.: G. Wilkinson, F. G. A. Stone, E. W. Abel), Pergamon Press, Oxford, England, **1982**, vol. 6.
[23] J. S. Valentine, *Chem. Rev.* **1973**, *73*, 235.
[24] M. Laing, M. J. Nolte, E. Singleton, *J. Chem. Soc., Chem. Commun.* **1975**, 660.
[25] A. Nakamura, Y. Tatsuno, M. Yamamoto, S. Otsuka, *J. Am. Chem. Soc.* **1971**, *93*, 6052.
[26] P. S. Pregosin, L. M. Venanzi, *Chem. Ber.* **1978**, *14*, 276.
[27] C. Eaborn, N. Farrell, J. L. Murphy, A. Pidcock, *J. Chem. Soc., Dalton Trans.* **1976**, 58.
[28] T. H. Brown, P. J. Green, *J. Am. Chem. Soc.* **1970**, *92*, 2359.
[29] C. A. Ghilardi, S. Midollini, S. Moneti, A. Orlandini, G. Scapacci, *J. Chem. Soc., Dalton Trans.* **1992**, 3371.
[30] T. E. Nappier, Jr., D. W. Meek, *J. Am. Chem. Soc.* **1972**, *94*, 306.
[31] T. J. Mazanec, PhD Dissertation, The Ohio State University, Columbus, OH, Dec. **1978**.
[32] J. A. McGinnety, N. C. Payne, J. A. Ibers, *J. Am. Chem. Soc.* **1969**, *91*, 6301.
[33] C. Bianchini, A. Meli, M. Peruzzini, F. Vizza, *J. Am. Chem. Soc.* **1990**, *112*, 6726.
[34] M. J. Nolte, E. Singleton, M. Laing, *J. Am. Chem. Soc.* **1975**, *97*, 6396.
[35] P. Barbaro, C. Bianchini, F. Laschi, S. Midollini, S. Moneti, G. Scapacci, P. Zanello, *Inorg. Chem.* **1994**, *33*, 1622.
[36] S. Sakaki, K. Hori, A. Ohyoshi, *Inorg. Chem.* **1978**, *17*, 3183.
[37] C. Yang, S. M. Socol, D. J. Kountz, D. W. Meek, R. Glaser, *Inorg. Chim. Acta* **1986**, *114*, 119.
[38] T. Hayashi, T. Mise, M. Fukushima, M. Kagotani, N. Nagashima, Y. Hamada, A. Matsumoto, S. Kawakami, M. Konishi, K. Yamamoto, M. Kumada, *Bull. Chem. Soc. Jpn.* **1980**, *53*, 1138.
[39] G. Giordano, R. H. Crabtree, *Inorg. Synth.* **1990**, *28*, 88.
[40] R. Cramer, *Inorg. Synth.* **1990**, *28*, 86.
[41] J. A. McCleverty, G. Wilkinson, *Inorg. Synth.* **1990**, *28*, 84.
[42] A. Van der Ent, A. L. Onderderlinden, *Inorg. Synth.* **1990**, *28*, 92.
[43] M. F. Summers, L. G. Marzilli, A. Bax, *J. Am. Chem. Soc.* **1986**, *108*, 4285.
[44] [44a] V. Sklener, H. Miyashiro, G. Zon, H. T. Miles, A. Bax, *FEBS Lett.* **1986**, *208*, 94. [44b] J. Jeener, B. H. Meier, P. Bachmann, R. R. Ernst, *J. Chem. Phys.* **1979**, *71*, 4546.

Received August 19, 2002
[I02469]